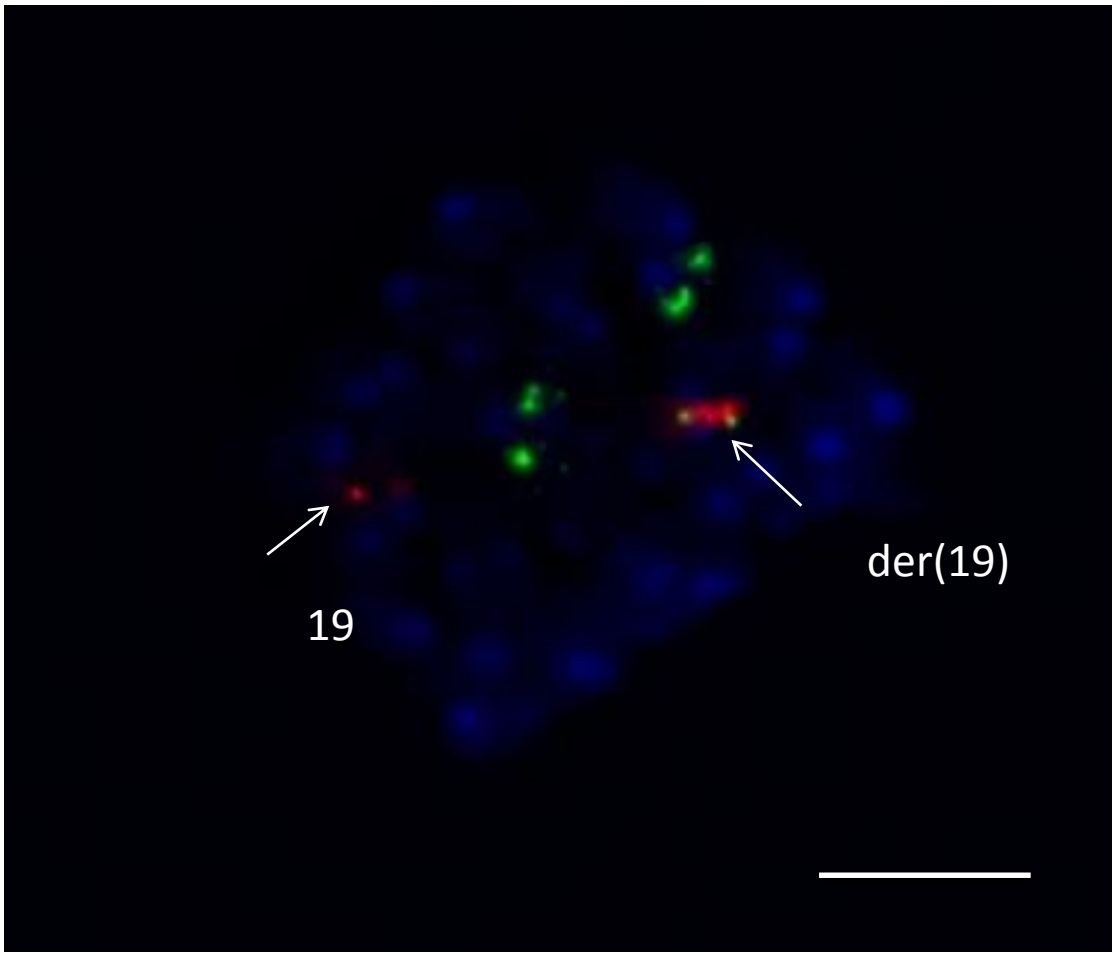


Supplementary Figure 1. BAC metaphase FISH on E***μ***-*Myc* transgenic cultured bone marrow cells. BAC RP23-307D14 (spectrum green) spans the MYC locus on chromosome 15. BAC RP23-324L2 (spectrum orange) spans JAK2 on chromosome 19. There is an extra, half strength green signal (MYC) co-localising with a red signal (Jak2) on the derivative chromosome 19 confirming that the transgene is located on chromosome 19. The red signal on the derivative 19 is always larger than the signal on the intact chromosome 19 which would support the presence of copy number gain in the region spanned by RP-324L2 but copy number cannot be accurately quantified. Scale bar = 10μm.

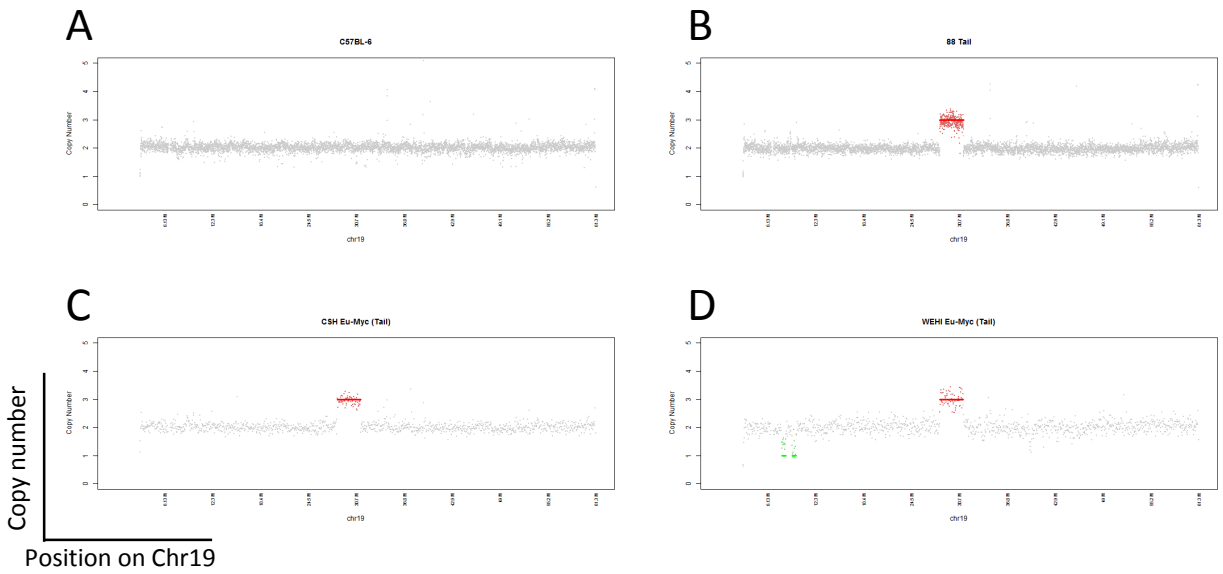


Supplementary Figure 2. Whole genome sequencing copy-number analysis highlighting germline amplification of the Chr19 segment proximal to E***μ***-*Myc* transgene insertion. A) C57BL/6 WT control B) E*μ-Myc* Peter MacCallum Cancer C) E*μ-Myc* Cold Spring Harbor D) E*μ-Myc* WEHI.

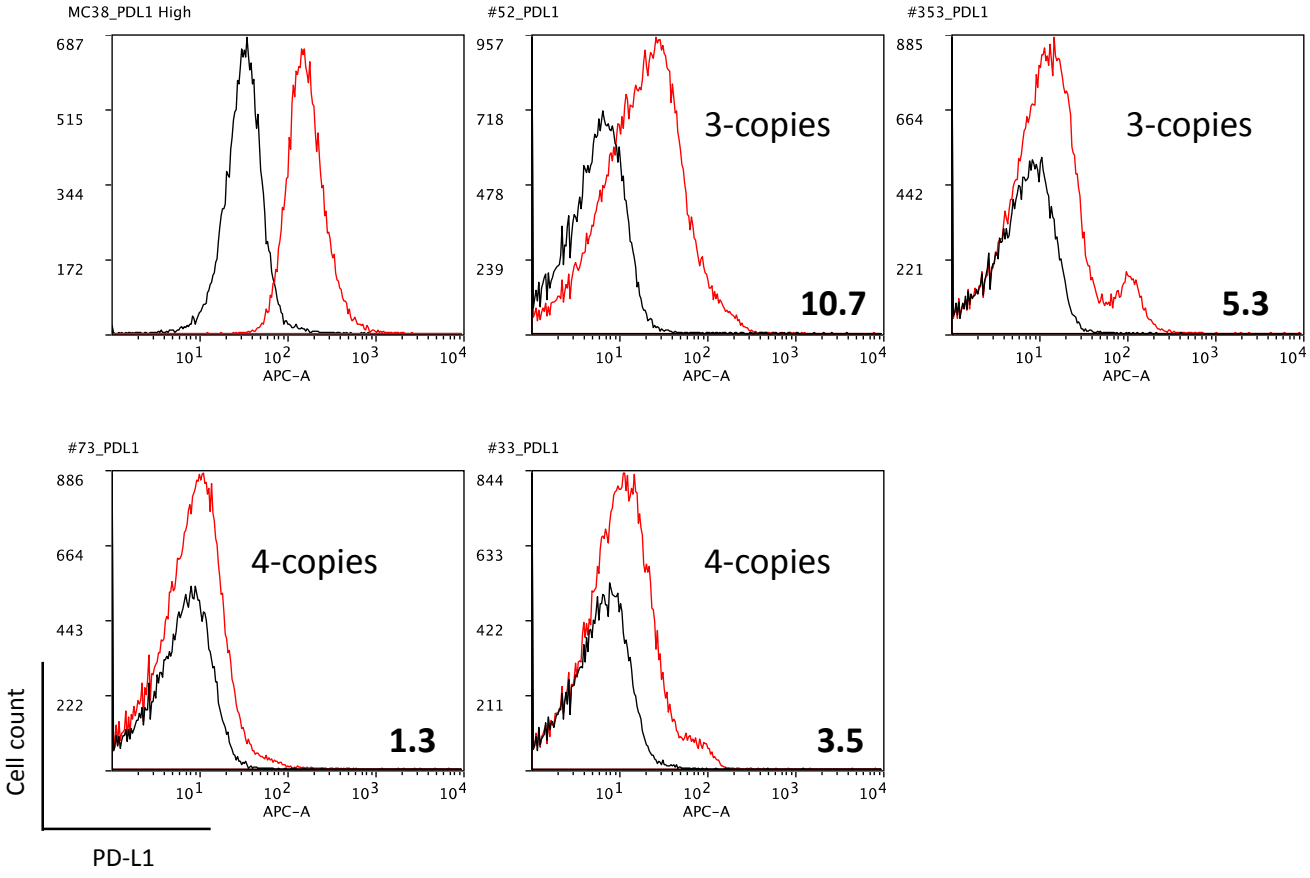


Supplementary Figure 3. FACS analysis of PD-L1 expression in E***μ***-*Myc* lymphomas shown to have varying *Cd274* (PD-L1) genomic copy-number. MC38 is a murine colorectal carcinoma cell line and PD-L1(Hi) control. #52 and #353 harbour 3-copies, #73 and #33 harbour 4 copies. Viable cells were gated based on morphology and CD220 positivity (not shown). Rat IgG2α isotype control (black), PD-L1 streptavidin APC - biotin APC Cy7 (red), difference in geometric mean fluorescence intensity for PDL1 fluorochrome compared to isotype control (bold text).

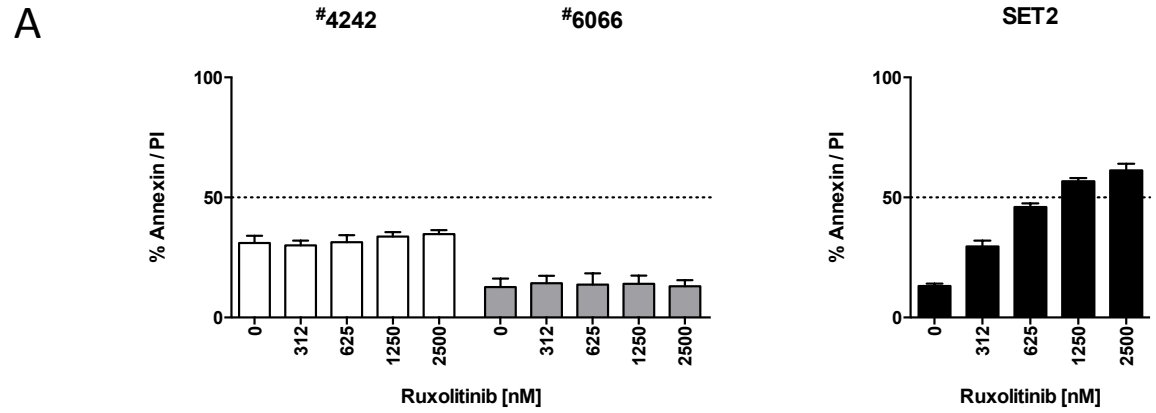


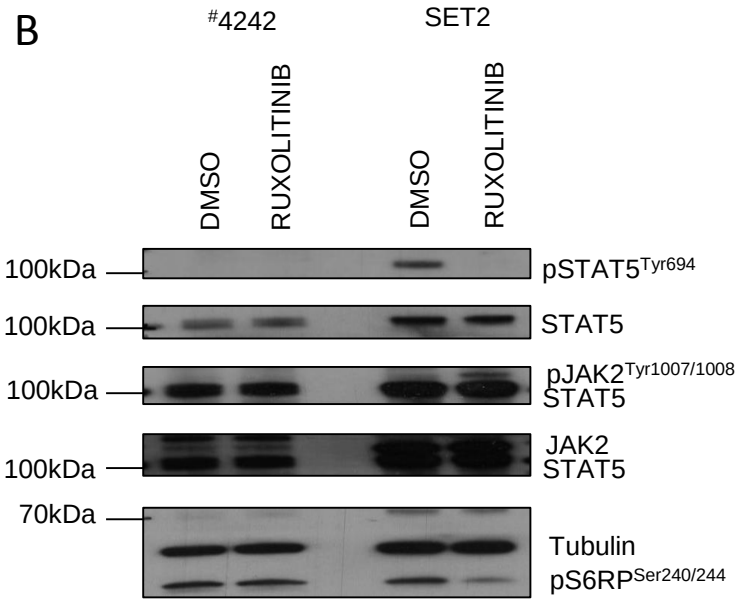


Supplementary Figure 4. JAK2 inhibition with ruxolitinib is insufficient to effect apoptosis of E***μ***-*Myc* lymphoma. A) E*μ-Myc* lymphomas #4242 and #6066 (left) were cultured in the presence of doubling dilutions of ruxolitinib for 24 hours prior to flow cytometric analysis for annexin-V / propidium iodide uptake. Human SET2(V617F) cell line (right) was used as positive control for ruxolitinib, cultured in RPMI media with doubling dilutions of ruxolitinib for 48 hours prior to flow cytometric analysis for annexin-V / propidium iodide uptake. Data shown is mean annexin-V/PI positive population ± SEM for triplicate experiments. B) E*μ-Myc* lymphoma #4242 and human SET2(V617F) cell lines were exposed to 1uM ruxolitinib or DMSO vehicle control for three hours prior to protein extraction and separation with SDS-PAGE. Immunoblotting was performed to show expression of pSTAT5, STAT5, pJAK2, JAK2, pS6RP and tubulin loading control.

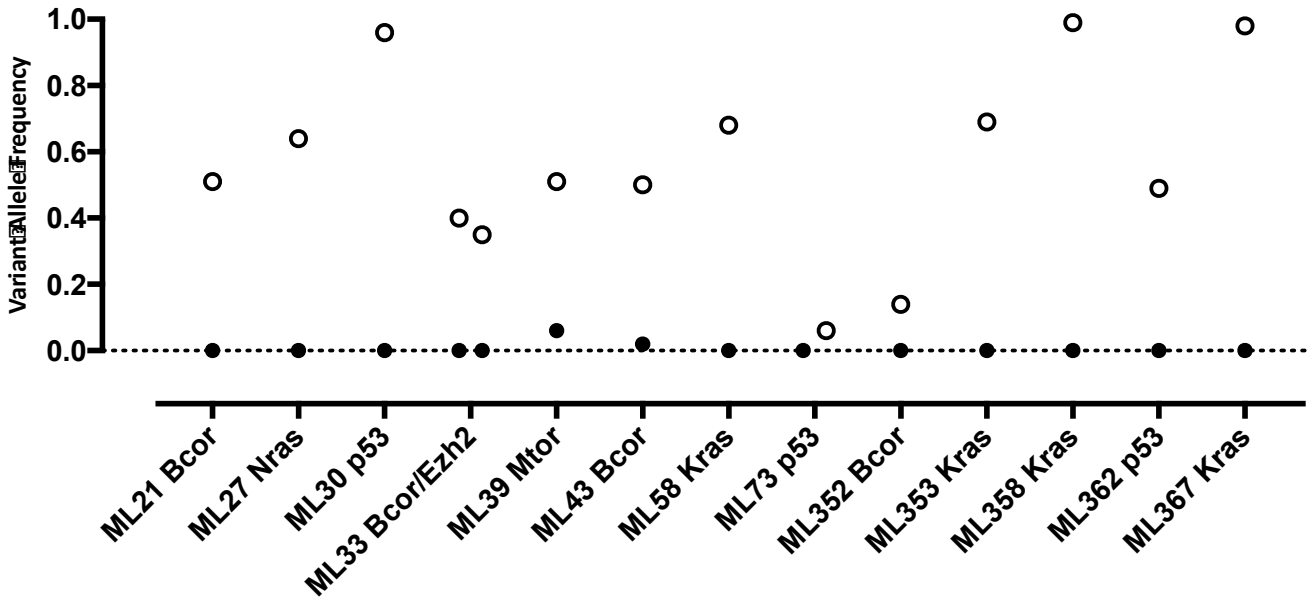


Supplementary Figure 5. Variant allele frequency determined by targeted amplicon sequencing. Targeted amplicon sequencing (TAM-seq) was performed on DNA extracted from peripheral blood at 4-weeks of age (filled circles) and at end-stage (empty-circles) to validate somatic mutations in E*μ-Myc* lymphomas. Candidate driver mutations were either undetectable or present at very low frequencies (<0.1) at 4-weeks of age and in each case were found at increased levels at end-point.

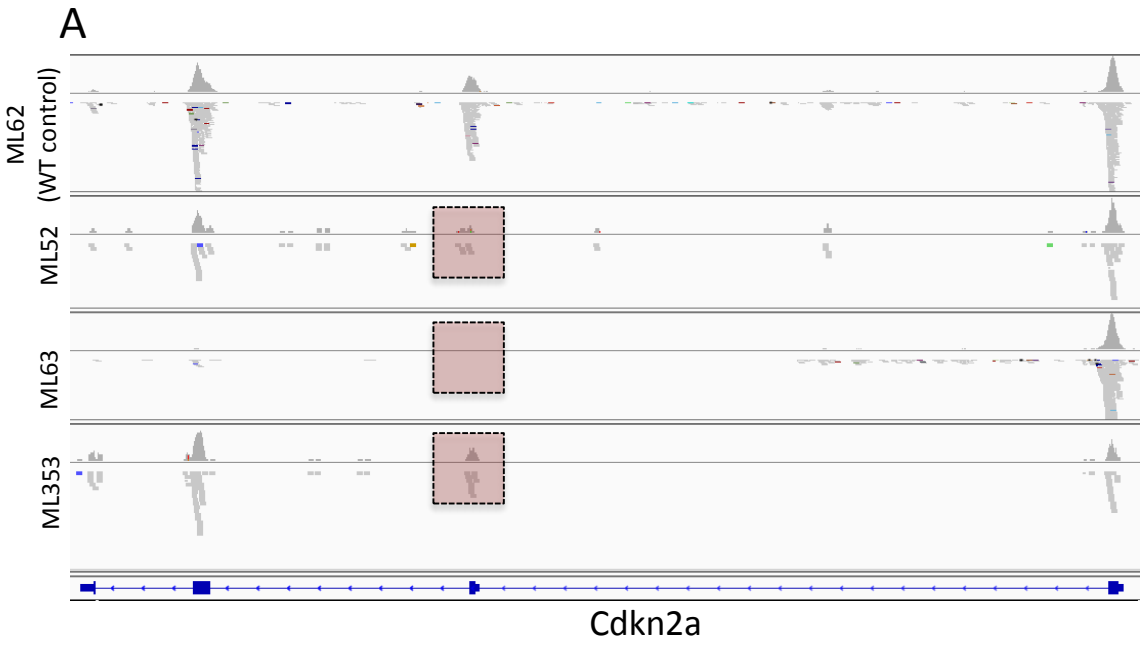


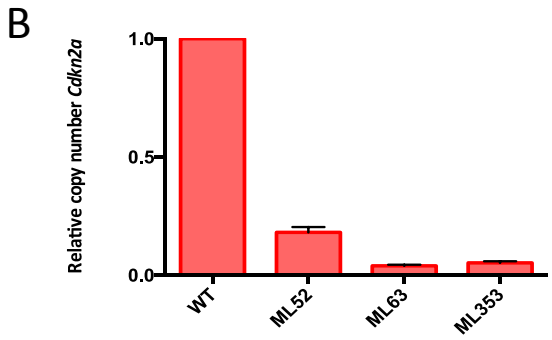


Supplementary Figure 6. Identification of focal deletions in cdkn2a. A) Whole exome sequencing analysis of read-pile up across the *Cdkn2a* locus showing potential *Cdkn2a* loss in ML52, ML63 and ML535 compared with WT littermate control (ML62). Dotted boxes indicate areas of reduced read depth indicative of copy number loss B) QRT-PCR displaying relative copy number for *Cdkn2a* confirms *Cdkn2a* deletion in ML52, ML63 and ML353 compared to WT littermate control (ML62). Data shown is mean relative copy number ± SEM, three replicates.

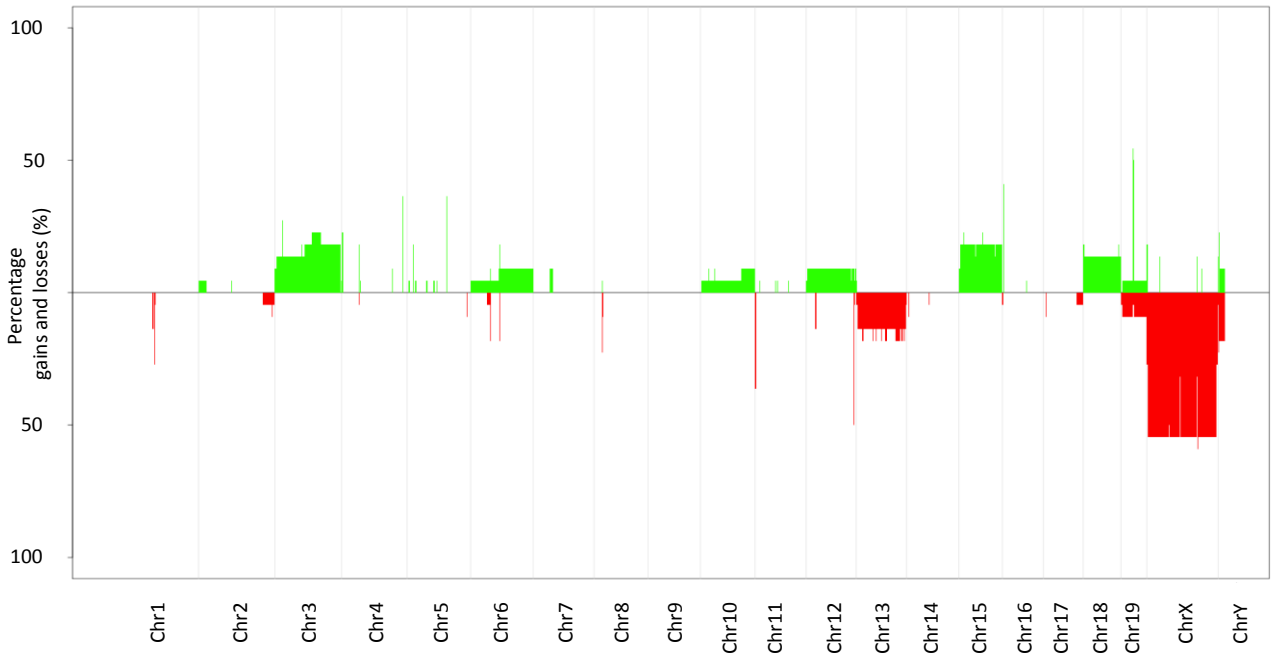


Supplementary Figure 7. Somatic copy-number alterations detected in Eμ-*Myc* lymphomas by whole-exome or low to medium coverage whole-genome sequencing. Overlapping regions of gain (green) or loss (red), are shown as a percentage of cases (22 cases analyzed) and are plotted against genome position (chromosome number).

A

| Well | Cell line | Barcode |
|---|---|---|
| A1 | 4242 | GTCTGAATGAAGTCGA |
| A4 | 4242 | CTCTGTGCGAGGAATT |
| C2 | 4242 | CTAGCTGTCTGCTGCG |
| D2 | 6066 | CAATCAGTGAGGTAGA |
| D11 | 6066 | CACTGTATCAAAGATA |
| F8 | 6066 | GTCGCTATGACACATA |

B

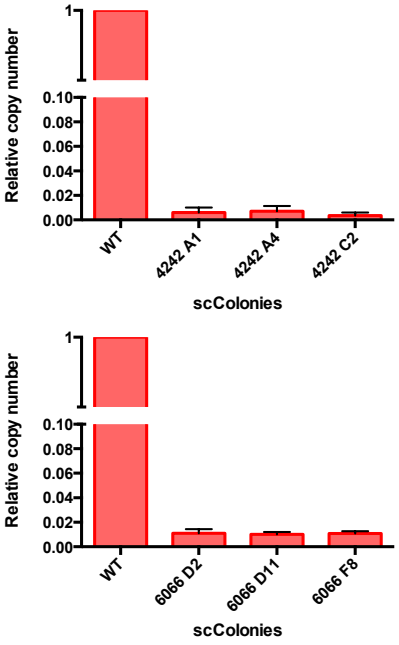


C

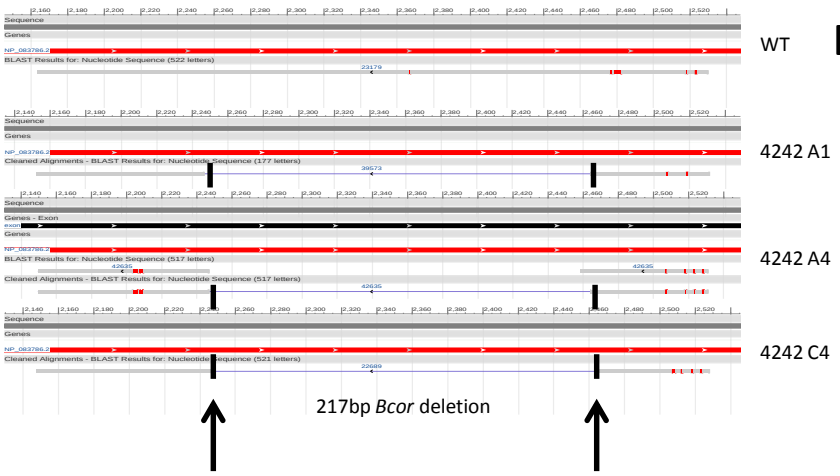


D

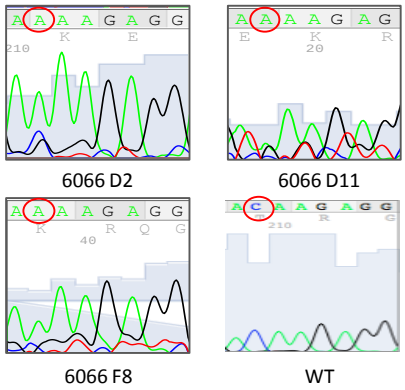


Supplementary Figure 8. Validation of coalescing driver mutations in #4242 and #6066 E***μ***-*Myc* clones. Cell lines were retrovirally transduced with an inert DNA 'barcode' and BFP fluorescent reporter at an MOI of 0.1. The cells were single-cell sorted on BFP expression and cultured to generate single-cell-derived colonies (scColonies). A) scColonies were sanger sequenced to show the presence of one barcode. B) QRT-PCR was performed to show total lack of *Cdkn2a* copies relative to WT control. Data shown is mean relative copy number ± SEM, three replicates. C) Sanger sequencing was performed on the 4242 scColonies and a BLAST readout highlights the 217bp deletion in *Bcor* apparent in the 4242 compared to WT. D) Sanger sequencing across *Nras* confirms C-to-A mutation corresponding to Q61K point mutation in the 6066 scColonies compared to WT

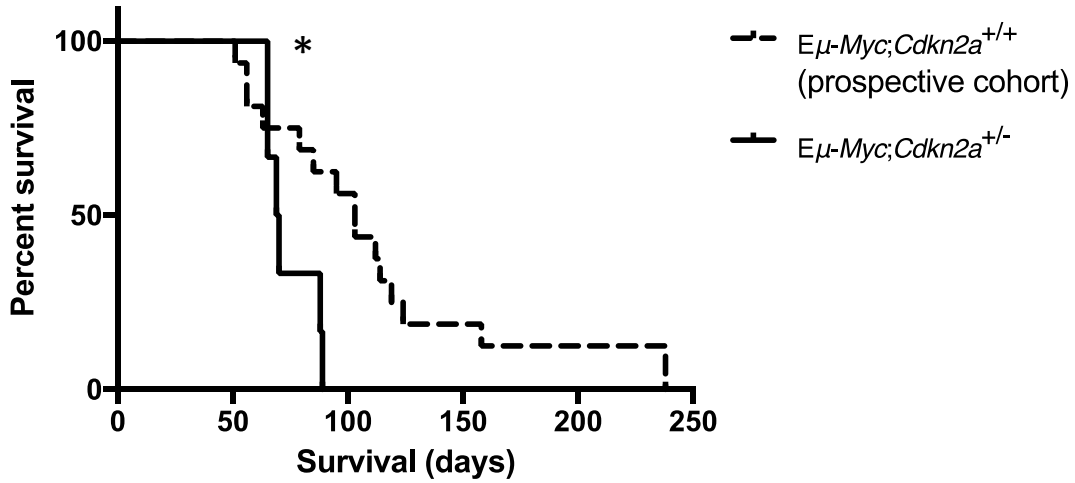


Supplementary Figure 9. E***μ***-*Myc*;*Cdkn2a*$^{+/-}$ mice have significantly accelerated mortality. Kaplan-Meier curve showing transgenic E*μ-Myc*;*Cdkn2a*$^{+/-}$ mice (solid line, n=6) and E*μ-Myc*;*Cdkn2a*$^{+/+}$ transgenic mice (dashed line, n=16), with a median survival time of 69.5 days and 103 days, respectively. * = p value < 0.05 log-rank (mantel-cox) test.

A

| GENE | CHR | POS | REF | ALT | CONSEQUENCE | REF DEPTH | ALT DEPTH | VAF |
|---|---|---|---|---|---|---|---|---|
| Kras | 6 | 123124 | T | G | Q61H | 58 | 37 | .67 |

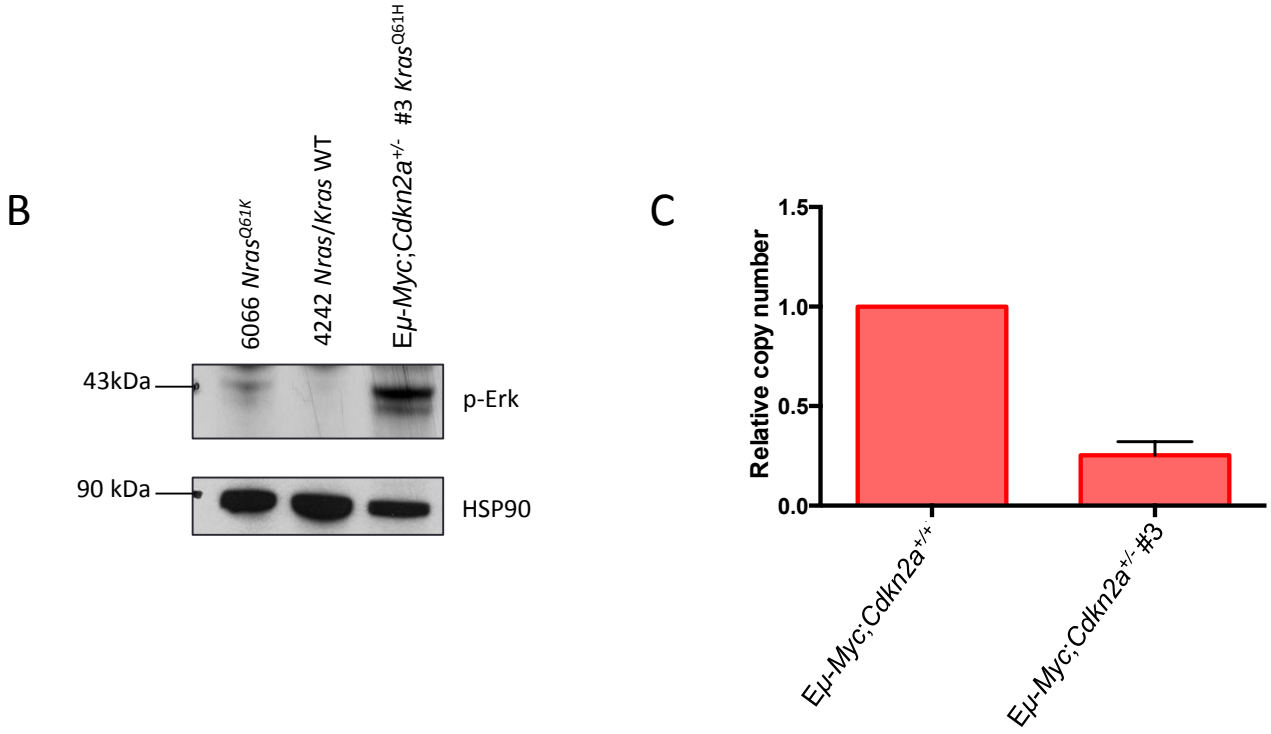


Supplementary Figure 10. Secondary and tertiary somatic mutations in E***μ***-*Myc*;*Cdkn2a*$^{+/-}$ lymphomas. A) Whole exome-sequencing readout showing the somatically acquired activating *Kras* mutation found in 1/6 E*μ*-*Myc*;*Cdkn2a*$^{+/-}$ lymphomas. B) Western blot analysis showing elevated phosphorylated ERK (p-ERK) in *Nras* mutant 6066 and E*μ*-*Myc*;*Cdkn2a*$^{+/-}$ #3 lymphoma indicating activated RAS MAPK pathway signaling. C) QRT-PCR analysis of the *Cdkn2a* locus in lymphoma E*μ*-*Myc*;*Cdkn2a*$^{+/-}$ #3 showing somatic deletion compared to E*μ*-*Myc*;*Cdkn2a*$^{+/+}$. Data shown is mean relative copy number ± SEM, three replicates.

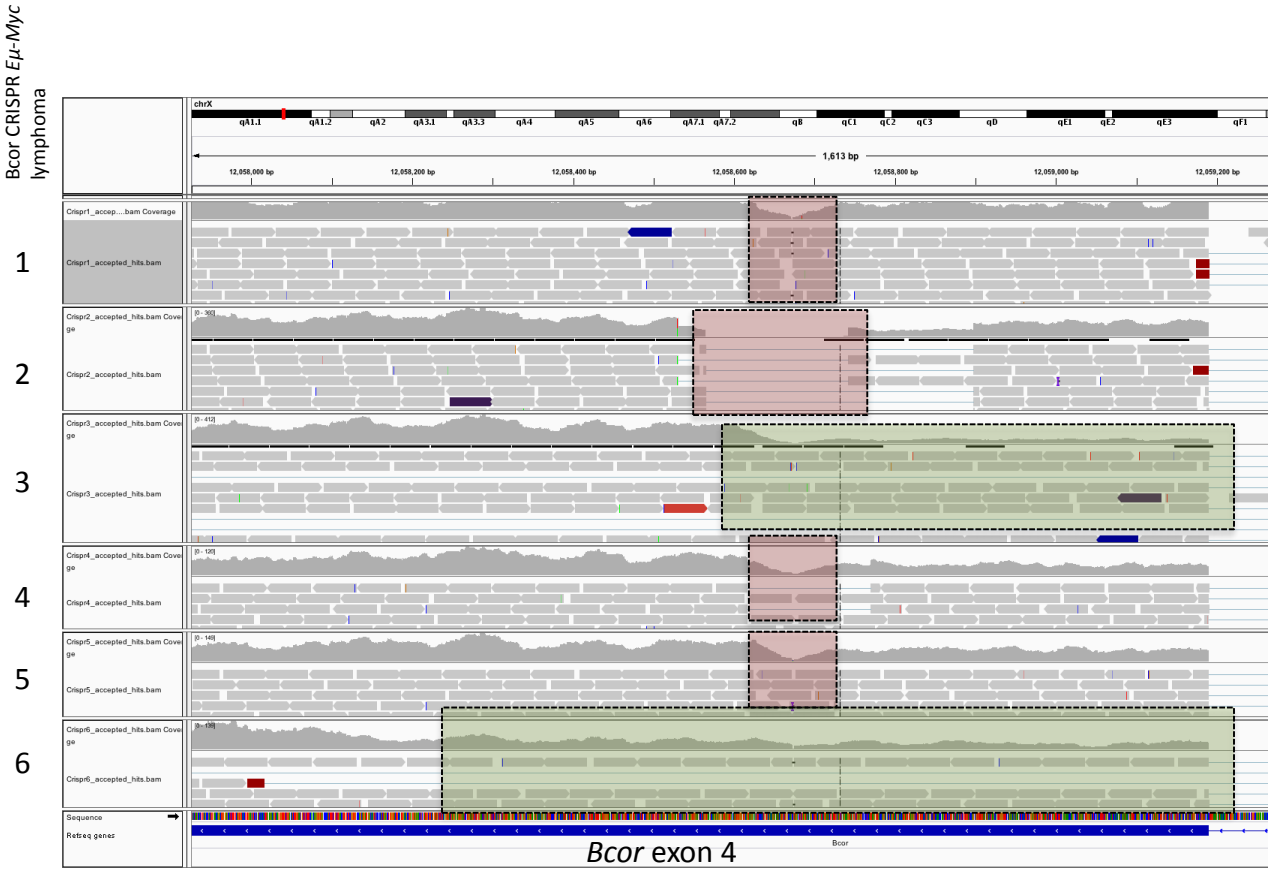


Supplementary Figure 11. RNA-seq IGV browser view showing CRISPR-Cas9 mediated *Bcor* insertions and deletions in E***μ***-*Myc* lymphomas. Red boxes represent small deletion events and green boxes represent reduced read depth, likely due to a large deletion event.

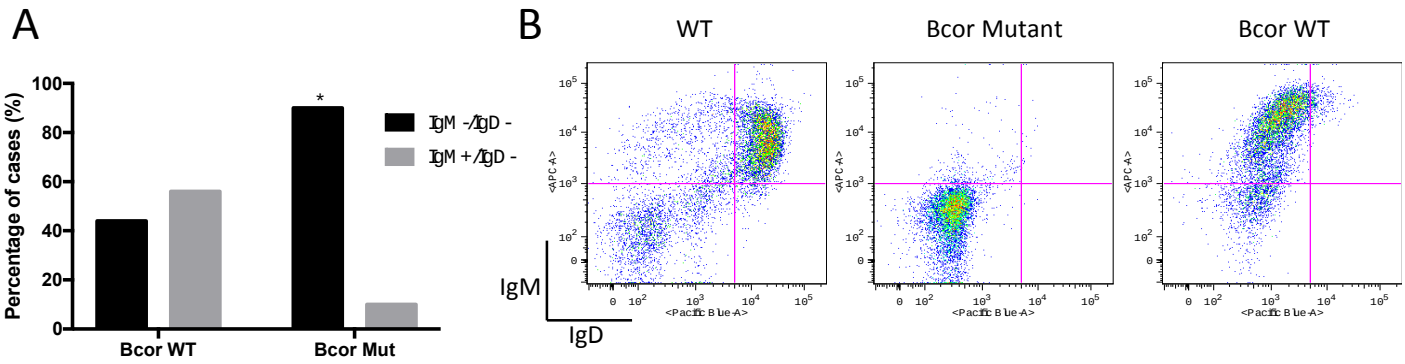


Supplementary Figure 12. Surface immunoglobulin profile of B-cells in *Bcor* mutant and *Bcor* WT sporadic and fetal liver cell-derived E***μ****-Myc* tumours. A) Surface IgM and IgD were assessed in the prospective E*μ-Myc* cohort (four *Bcor* mutant tumours and 12 *Bcor* WT tumours) and 12 fetal liver derived E*μ-Myc* tumours (six *Bcor* mutant tumours (*Bcor* KD) and six *Bcor* WT tumours (p53 KD)). 90% of *Bcor* mutant tumours were IgM-/IgD- while 10% were IgM+/IgD-. 44.4% pf *Bcor* WT tumours were IgM-/IgD- while 56.6% were IgM+/IgD-. *Bcor* mutations are associated with an IgM-/IgD- profile (Chi-squared test, $p<0.05$). B) Representative IgM/IgD FACS plots showing WT bone marrow B-cells, Bcor mutant E*μ-Myc* tumour cells and *Bcor* WT E*μ-Myc* tumour cells.

A

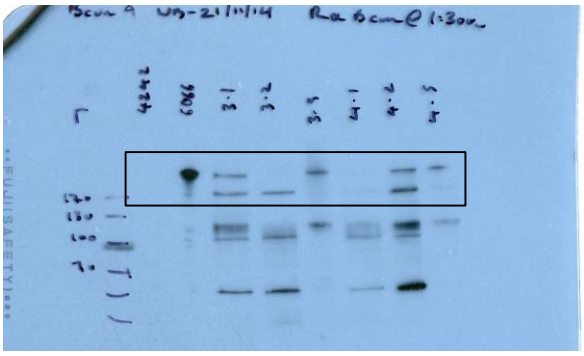

B

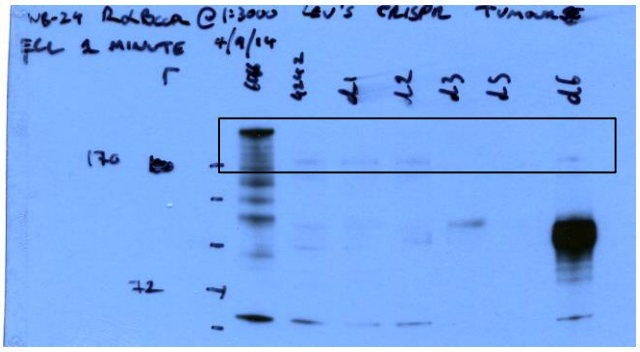

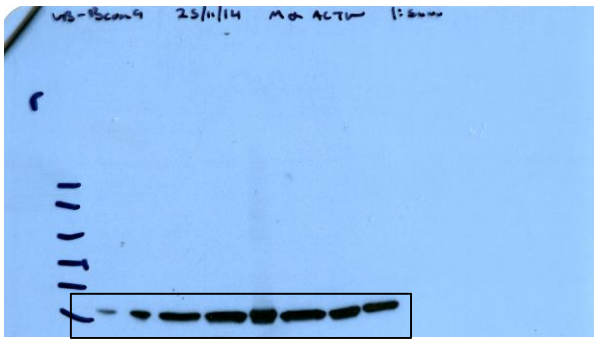

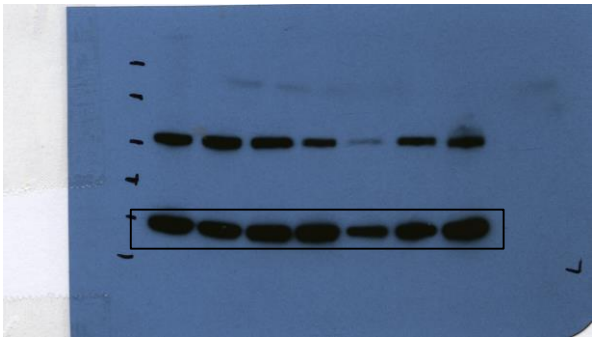

Supplementary Figure 13. Unedited western blots shown in main Figure 4. Black boxes correlate with the edited images shown in the main text. A) Original blots shown in Figure 4D and B) Original blots shown in Figure 4E.

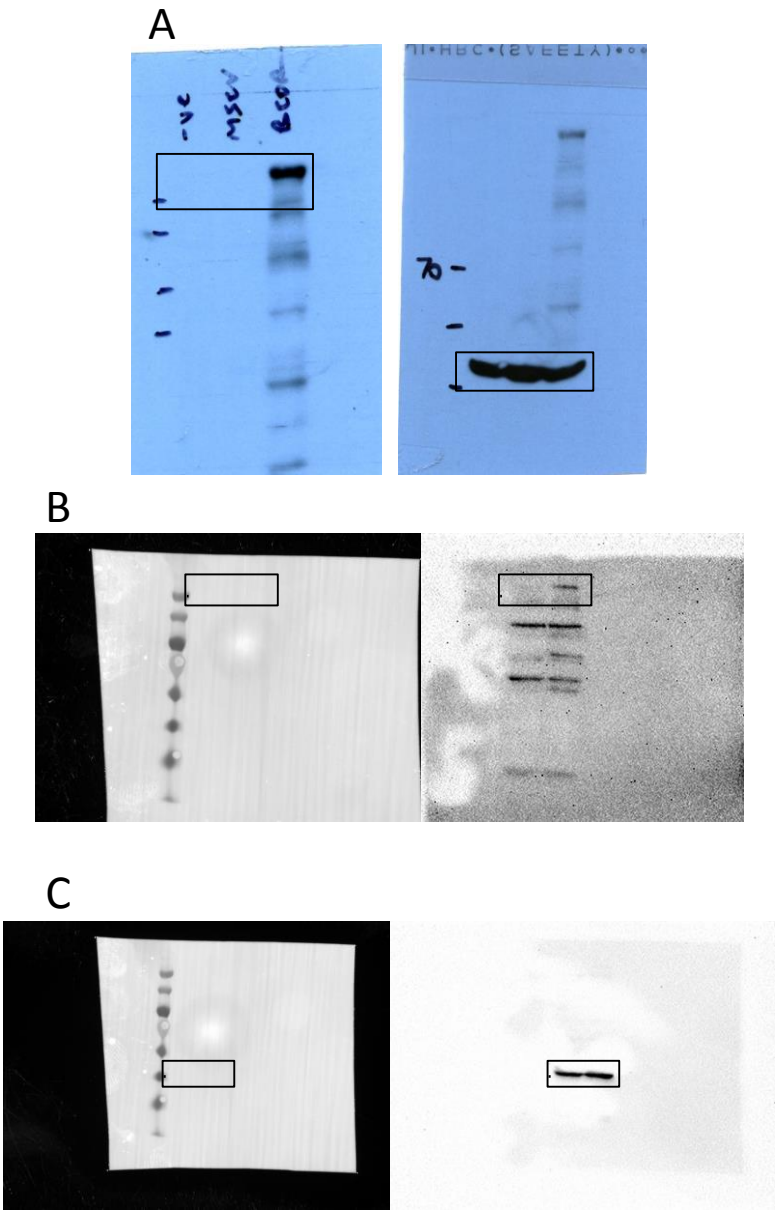


Supplementary Figure 14. Unedited western blots shown in main Figure 5. Black boxes correlate with the edited images shown in the main text. A) Original blots shown in Figure 5B, B) Original blots shown in Figure 5D upper-panel and C) original blots shown in Figure 5D lower-panel. For B) and C) western blots were imaged using the BioRad Chemidoc, which provides colorimetric images (protein ladder) and chemiluminescent images (protein bands) from which a composite image can be made giving molecular weight estimates against protein bands.

**Supplementary Table 1.** Summary of Eu-Myc mice and disease presentation

| ID | Sex | Latency (days) | Generation | Relation ship | IgM/IgD profiles | WBC (10^9 cells/L) | Presentation |
|---|---|---|---|---|---|---|---|
| ML20 | F | 124 | Prospective B | Father 371 | IgM lo IgD- / IgM hi IgD- | 108.2 | Splenic/thymic |
| ML21 | F | 119 | Prospective B | Father 371 | IgM- IgD- | 34.2 | Splenic/Nodal |
| ML27 | F | 51 | Prospective B | Father 371 | IgM lo IgD- | 121.6 | Splenic/Nodal |
| ML30 | F | 95 | Prospective B | Father 371 | IgM- IgD- | 49.4 | Splenic/Nodal |
| ML33 | F | 103 | Prospective B | Father 371 | IgM- IgD- | 64.8 | Splenic/Nodal |
| ML39 | F | 168 | Prospective B | Father 371 | IgM- IgD- | 45.2 | Splenic/Nodal |
| ML43 | F | 79 | Prospective B | Father 371 | IgM- IgD- | 50.4 | Splenic/Nodal |
| ML52 | F | 85 | Prospective B | Father 371 | IgM hi IgD- | 461.4 | Thymic/Nodal |
| ML58 | M | 63 | Prospective B | Father 371 | IgM- IgD- | 158.8 | Splenic/Nodal |
| ML63 | M | 103 | Prospective B | Father 371 | IgM hi IgD- | 94 | Splenic/Nodal |
| ML73 | F | 114 | Prospective B | Father 371 | IgM lo IgD- / IgM hi IgD- | 145.2 | Splenic/Thymic |
| ML352 | F | 130 | Prospective A | Father 288 | IgM- IgD- | 5 | Splenic/Nodal |
| ML353 | F | 238 | Prospective A | Father 288 | IgM lo IgD- / IgM hi IgD- | 36.8 | Splenic/Nodal |
| ML358 | M | 56 | Prospective A | Father 288 | IgM- IgD- | 42.2 | Splenic/Nodal |
| ML362 | F | 56 | Prospective A | Father 288 | IgM hi IgD- | 65.8 | Splenic/Nodal |
| ML367 | M | 158 | Prospective A | Father 288 | IgM- IgD- | 94 | Splenic/Nodal |
| #4242 (cell line) | M | N/A | Retrospective | none | n/a | n/a | n/a |
| #6066 (cell line) | M | N/A | Retrospective | none | n/a | n/a | n/a |
| #299 | M | 126 | Retrospective | none | n/a | n/a | n/a |
| #88 | M | N/A | Retrospective | none | n/a | n/a | n/a |
| #13 | M | 189 | Retrospective | none | n/a | n/a | n/a |
| #218 | M | 218 | Retrospective | Brother 219 | n/a | n/a | n/a |
| #219 | M | 105 | Retrospective | Brother 218 | n/a | n/a | n/a |

**Supplementary Table 2.** shRNA and CRISPR-Cas9 sequences

| **Gene ID** | **Hairpin ID** | **Hairpin Sequence** |
|---|---|---|
| Bcor | Bcor9 | TGCTGTTGACAGTGAGCGACGAGAAGAAGCAGACACTAAATAGTGAAGCCACAGATGTATTTAGTGTCTGCTTCTTCTCGG TGCCTACTGCCTCGGA |
| trp53 | p53.1224 | CTCGAGAAGGTATATTGCTGTTGACAGTGAGCGCCCACTACAAGTACATGTGTAATAGTGAAGCCACAGATGTATTACACA TGTACTTGTAGTGGATGCCTACTGCCTCGGAATTC |
| n/a | scrambled | TGCTGTTGACAGTGAGCGATCTCGCTTGGGCGAGAGTAAGTAGTGAAGCCACAGATGTACTTACTCTCGCCCAAGCGAGA GTGCCTACTGCCTCGGA |
| | | |
| **Gene ID** | **crispr trigger ID** | **crispr trigger sequence** |
| Bcor | BcorG2 | CAGTGGCTGGGCCAAGCCGT |
| Trp53 | p53(b) | GAAGTCACAGCACATGACGG |